Available online at www.sciencedirect.com
ScienceDirect
Experimental Neurology 210 (2008) 95–108
Experimental Neurology
www.elsevier.com/locate/yexnr

Impact of neonatal asphyxia and hind limb immobilization on musculoskeletal tissues and S1 map organization: Implications for cerebral palsy

Jacques-Olivier Coq [a,*,1], Fabrizio Strata [b,2], Michaël Russier [a], Fayez F. Safadi [c], Michael M. Merzenich [b], Nancy N. Byl [d], Mary F. Barbe [c,e,1]

[a] UMR 6149 Neurobiologie Intégrative et Adaptative, Aix-Marseille Université–CNRS, Pôle 3C, Case B, 3 Place Victor Hugo, 13331 Marseille Cedex 03, France
[b] Keck Center for Integrative Neuroscience, University of California San Francisco, 513 Parnassus Avenue, San Francisco, California 94143-0732, USA
[c] Department of Anatomy and Cell Biology, 3400 North Broad Street, Temple Medical School, Philadelphia, PA, 19140, USA
[d] Department of Physical Therapy and Rehabilitation Science, School of Medicine, 1318 7th Ave. Box 0736, University of California, San Francisco, CA 94143-0736, USA
[e] Department of Physical Therapy, College of Health Professions, Temple University, 3307 North Broad Street, Philadelphia, PA 19140, USA

Received 3 July 2007; revised 18 September 2007; accepted 5 October 2007
Available online 24 October 2007

Abstract

Cerebral palsy (CP) is a complex disorder of locomotion, posture and movements resulting from pre-, peri- or postnatal damage to the developing brain. In a previous study (Strata, F., Coq, J.O., Byl, N.N., Merzenich, M.M., 2004. Comparison between sensorimotor restriction and anoxia on gait and motor cortex organization: implications for a rodent model of cerebral palsy. Neuroscience 129, 141–156.), CP-like movement disorders were more reliably reproduced in rats by hind limb sensorimotor restriction (disuse) during development rather than perinatal asphyxia (PA). To gain new insights into the underpinning mechanisms of CP symptoms we investigated the long-term effects of PA and disuse on the hind limb musculoskeletal histology and topographical organization in the primary somatosensory cortex (S1) of adult rats. Developmental disuse (i.e. hind limb immobilization) associated with PA induced muscle fiber atrophy, extracellular matrix changes in the muscle, and mild to moderate ankle and knee joint degeneration at levels greater than disuse alone. Sensorimotor restricted rats with or without PA exhibited a topographical disorganization of the S1 cortical hind limb representation with abnormally large, multiple and overlapping receptive fields. This disorganization was enhanced when disuse and PA were associated. Altered cortical neuronal properties included increased cortical responsiveness and a decrease in neuronal selectivity to afferent inputs. These data support previous observations that asphyxia per se can generate the substrate for peripheral tissue and brain damage, which are worsened by aberrant sensorimotor experience during maturation, and could explain the disabling movement disorders observed in children with CP.

Keywords: Perinatal asphyxia; Developmental disuse; Movement disorders; Hind paw; Muscle atrophy; Joint degeneration; Primary somatosensory cortex; Electrophysiological mapping

Introduction

Perinatal asphyxia (PA) remains a major cause of neonatal mortality and of permanent neurodevelopmental disability in children, including cerebral palsy (CP), seizure disorders and mental retardation in later life (Hill and Volpe, 1989; Vannucci et al., 1999). According to several studies, preterm birth, asphyxia before, during and after birth, and fetal and/or maternal infections entail a higher risk for CP (Hill and Volpe, 1989; Nelson and Grether, 1999; Haynes et al., 2005; Blomgren and Hagberg, 2006). Several animal models based on PA have reproduced brain damage found in patients with CP, such as periventricular white matter injury (e.g. Olivier et al., 2005; Blomgren and Hagberg, 2006). Only a few studies using

* Corresponding author. Fax: +33 488 576 800.
E-mail address: coqjo@up.univ-mrs.fr (J.-O. Coq).
[1] Denotes authors of equal contributions.
[2] Present address: Neuroscience Department, Physiology Section, University of Parma, Via Volturno 39/E, 43100 Parma, Italy.

0014-4886/$ - see front matter © 2007 Elsevier Inc. All rights reserved.
doi:10.1016/j.expneurol.2007.10.006

PA have reported spasticity in relation to degraded locomotion in monkeys (Myers, 1975) and rabbits (Derrick et al., 2004; Drobyshevsky et al., 2007), while hypertonic spasticity has been commonly described in animal models of disuse (e.g. Canu and Falempin, 1996; Bouet et al., 2003; Strata et al., 2004).

Normal infants produce a large and rich repertoire of spontaneous movements from early fetal life until the end of the first half of a year of life. In contrast, children with CP display scarce, monotonous and stereotypical patterns of cramped-synchronized spontaneous movements that lack complexity, variation, and fluency (Prechtl, 1997; Hadders-Algra, 2004; Einspieler and Prechtl, 2005). Deficits in these spontaneous movements could account for musculoskeletal tissue changes found in these children. Indeed, varying degrees of atrophy and hypertrophy of muscle fibers (Lindboe and Platou, 1982; Romanini et al., 1989; Rose et al., 1994; Marbini et al., 2002) and increased fat and connective tissue within muscles (Castle et al., 1979; Jarvinen et al., 2002) have been reported in children with spastic CP. These muscle changes could be responsible for abnormal forces on bones and joints resulting in secondary bone malformations (Banks, 1972; Gormley, 2001) and/or articular cartilage degenerative changes (Banks, 1972; Lundy et al., 1998). Moreover, musculoskeletal changes contribute to provide abnormal sensory inputs to the brain, resulting in repetitive, aberrant sensory feedback, deleterious somatosensory and motor cortical reorganization, and ultimately in degraded motor function. A recent study in humans has provided evidence of somatosensory cortex reorganization following perinatal brain injury and of the effects of motor impairments on tactile discrimination abilities of infants with CP (Clayton et al., 2003).

Recently, Strata et al. (2004) developed a rodent model to reproduce the motor deficits observed in children with CP. Rats exposed to PA exhibited subtle motor behavioral anomalies and alterations of the representation of hind limb movements in the primary motor cortex (M1). While PA alone did not induce spasticity or degraded motor function in adult rats, hind limb immobilization (i.e. disuse) during development with or without PA, resulted in increased muscular tone at rest and during active flexion or extension, abnormal walking patterns in open-field, on a suspended bar, or on a rota-rod. These restrained rats also displayed a degraded M1 representation of hind limb movements.

Most of the studies on animal models of CP focus on brain damage and/or motor deficits (e.g. Bernert et al., 2003; Derrick et al., 2004; Drobyshevsky et al., 2007; Kohlhauser et al., 1999, 2000; Olivier et al., 2005; Van de Berg et al., 2000, 2003; see Vannucci et al., 1999 for review), but not on sensory deficits and peripheral tissues changes, even though somatosensory inputs and musculoskeletal integrity are essential components of motor function, control and development. As part of a broad effort to understand the role of early brain injuries and/or disuse on musculoskeletal system and brain network development, the present study examines the hind limb muscle and joint histology and the topographical organization of the primary somatosensory cortex (S1) in sensorimotor restricted rats with or without exposure to PA. Our results show that PA alone induces almost no effects on both peripheral tissues and S1 hind limb maps compared to control rats. In contrast, the sensorimotor restriction alone had deleterious effects on musculoskeletal histology and S1 map organization. Interestingly, the combination of PA and hind limb immobilization had the most deleterious impacts. These results contribute to gain new insights into the generation of movement disorders in human cerebral palsy.

Materials and methods

Subjects

Twenty eight newborn Sprague–Dawley rats from either sex were randomly assigned to 4 groups: 1) controls (CONT, $n=7$); 2) asphyxiated at birth (PA, $n=7$); 3) sensorimotor restricted during development (SR, $n=6$); and 4) asphyxiated at birth and sensorimotor restricted (PA+SR, $n=8$). All rats had water and food ad libitum, and were maintained in a 12-h light–dark cycle. The floor of all cages was covered with sawdust. All experiments were carried out in accordance with the guidelines laid down by the NIH and all animal use was approved by the Committee on Animal Research at the University of California at San Francisco.

Neonatal asphyxia

Pups from different litters experienced two episodes of asphyxia (PA) for 12 min each at the day of birth (P0) and on P1. The pups were placed on a thermal blanket (37.5 °C) in a plexiglas airtight chamber with two valves (Vetequip, Pleasanton, CA). Atmospheric nitrogen (N_2) gas was passed through the inlet valve until complete asphyxia occurred (Buwalda et al., 1995). Lowering the atmospheric oxygen concentration in the chamber resulted in hyperactivity of the pups, followed by a loss of movement, sporadic gasping and a change of skin color from pink to bluish. After each episode of asphyxia, pups were removed from the chamber to be kept in normal atmospheric conditions until they recovered their original skin color, normal breathing and postural reflexes. They were then returned to their mother. Atmospheric air was used for control and SR rats.

Sensorimotor restriction

Rats belonging to SR and PA+SR groups were restrained for 16h per day from P2 to P28. Pups' feet were gently bound together with medical tape, and their hind limbs were immobilized in an extended position with a cast made of hand-moldable epoxy putty stick (see Supplemental Fig. 1), which allowed only limited movements around the hip joint (see Fig. 1 in Strata et al., 2004, for more details). Casts did not prevent pups to urinate, defecate and to receive maternal cares. After casting, pups were returned to their mother and unrestrained littermates. The restrained rats were allowed to move freely for 8h per day. The casting was simulated in unrestricted rats without taping their hind limbs, so that all rats received similar handling. The size of the casts was adapted to the growth of the rats from P2 to P28. Body growth of restrained pups was significantly lower than that of unrestricted rats from the same litters (see Strata

et al., 2004 for details). The differences in body growth between restricted and unrestrained rats decreased over time after the ending of sensorimotor restriction (Strata et al., 2004). The possible impact of stress induced by the casting and hind limb immobilization was minimized by similar handling of all groups of rats (Meaney et al., 1989; Durand et al., 1998).

Electrophysiological mapping procedures

All groups of rats were subjected to gait analysis and motor skill evaluation once a week from P17 to P45 (see Strata et al., 2004). Seven controls (CONT), 7 asphyxiated (PA), 6 sensorimotor restricted (SR) and 6 asphyxiated and restricted (PA+SR) rats underwent electrophysiological recordings at ages P46 to P99. Rats were anesthetized with sodium pentobarbital (50 mg/kg, i.p.) and supplemental doses (5 mg/kg, i.p.) delivered as needed to maintain a surgical level of anesthesia. Repeated injections of atropine (0.1 mg/kg, i.m.) and lactated Ringers solution allowed animals to be kept in stable physiological conditions during mapping sessions. Rectal temperature was monitored and maintained near 37.5 °C with a thermostatically controlled heating pad.

A craniotomy was made over the S1 cortex of the left hemisphere corresponding to the hind limb representation. After dura mater resection, the cortical surface was covered with a thin layer of silicone fluid to prevent drying. An enlarged digital image of the exposed brain surface was used to guide and record the location of electrode penetrations in MAP software (Peterson and Merzenich, 1995; Supplemental Fig. 2A). Multiunit recordings were made with tungsten microelectrodes (WPI, 1 MΩ at 1 kHz) introduced perpendicular to the cortical surface. Sites of electrode penetration were identified relative to the vasculature of the cortical surface. The interelectrode penetration distance ranged from 50 to 100 μm and was roughly similar for all groups of rats. The recording artifact generated by the microelectrode contact with the cortical surface was used to set a zero level. The electrode was advanced into the cortex using a hydraulic microdrive (David Kopf Instruments, Tujunga, CA) and receptive fields (RFs) were determined in the putative upper layer IV (650–800 μm) of the S1 cortex.

The mapping procedure used in the present study has been described in detail in previous papers (e.g. Coq and Xerri, 1999). Briefly, the multiunit signal was preamplified, filtered (bandpass: 0.5–5 kHz), displayed on an oscilloscope, and delivered to an audio monitor. At each recording site, cortical responses produced by natural stimulation were readily detected by large bursts of activity (see Fig. 2A in Coq and Xerri, 1999 for details). Low-threshold cutaneous RFs were defined using hand-held probes or brushes to produce light skin indentations or gentle hair movements, respectively. High-threshold cortical sites were classified as non-cutaneous responses elicited by taps on skin and stroking hairs. Responses to manipulations of muscles and joints were presumed to be related to deep receptors. Responses evoked by nail movements were examined while the tips of the toes were firmly maintained to minimize joint movement and skin deformation. Cortical responsiveness to somatic stimuli was classified along a 3-level scale (weak, good and excellent responses) on the basis of the magnitude of the signal-to-noise ratio. Cortical sites that did not exhibit stimulus-evoked responses, but spontaneous discharges only were classified as unresponsive.

The ridges running along the glabrous skin of the toes and sole were used as reliable landmarks to delineate and draw the RFs (see Supplemental Fig. 2B). The RF areas were transferred to the digital image of the hind paw and were subsequently measured offline using MAP software. We used Canvas software (Deneba) to elaborate maps of the hind limb representation by drawing boundaries encompassing cortical sites whose RFs were restricted to a common hind limb subdivision (e.g. toe, plantar pad, heel, leg). Borders were drawn midway between adjacent recording sites whose RFs were located on distinct and separate skin subdivisions. A boundary line crossed cortical sites with two distinct, multiple RFs or with single RF located on different but adjoining skin subdivisions of the hind limb. Cortical penetrations with single or multiple RFs that encompassed three or more foot subdivisions (e.g. two toes and a pad) were pooled together. Map borders were placed midway between responsive and unresponsive sites. The investigator mapping the hind paw representation was unaware of the experimental conditions of the animal throughout the recording session. The reproducibility of RF delineation and map elaboration was frequently checked between experimenters.

Tissue collection, histology and immunochemistry

Lower extremity tissues were examined for histological changes in 7 control, 6 PA, 4 SR, and 8 PA+SR rats. At the end of each mapping experiment, rats were euthanized by pentobarbital overdose (150 mg/kg, i.p.), perfused transcardially with 4% paraformaldehyde in 0.1 M phosphate buffer (pH 7.4), and hind limbs collected and postfixed by immersion for 2–3 days. Skeletal tissues were dissected away from musculotendinous tissues. The knee and ankle joints were paraffin embedded, cut into 5 μm longitudinal sections and mounted onto coated slides (Fisher Plus). These sections were stained with hematoxylin and eosin (H&E) or immunohistochemically (see below). The following muscles were collected from each hind limb: gluteus maximus, quadriceps femoris, hamstrings, and triceps surae. These tissues were equilibrated for 3 days in 30% sucrose in phosphate buffer (pH 7.4), cut into 16μm longitudinal sections using a cryostat, mounted onto coated slides, and stored at −80 °C until stained with H&E or immunohistochemically. The gluteus maximus muscles were examined only for immunohistochemical analysis since longitudinal plane only sections were more difficult to obtain from this muscle. Immunohistochemical analysis for collagen type I and connective tissue growth factor (CTGF) was performed on the tissues using the methods described previously (Clark et al., 2004).

Hind limb morphometry

To assess the treatments on muscle fiber size, diameter measurements of individual myofibers were performed, in a

blinded fashion, using a bioquantification system (Bioquant TCW98) interfaced with a Nikon microscope. A total of 35 to 50 myofibers were measured per muscle in 3 non-adjacent sections using 400× magnification, bilaterally. Group means and standard errors (SEM) of myofiber diameters were determined for each muscle per group. Bin frequency histograms (10 μm per bin) of the triceps surae myofiber diameters were generated from the raw myofiber diameter data for each group.

To determine the effect of treatment on CTGF and collagen type I production in muscles, immunofluorescence stained slides were quantified for percent area occupied by immunostaining using the methods described previously (Clark et al., 2004). Three non-adjacent sites were measured per muscle, bilaterally. The sampling strategy used involved analyzing frames in the medial, lateral and middle regions of each muscle belly at 400× magnification. Right and left limb results were averaged together. Group means and SEM of the percent area fraction of immunostaining were determined for each muscle per group.

H&E and CTGF stained joint sections were examined qualitatively for histopathological changes. The articular cartilage of the knee and ankle joints was histologically assessed, in a blinded manner, using a classification system described by Yamamoto et al. (2005) based on Maier's system. The severity of articular cartilage degeneration was classified into 5 stages: stage 0, normal; stage I, damage in the superficial cartilage layer, e.g. eburnations or thickenings of this layer; stage II, defects (e.g. thinning) in the cartilage down to the tidemark; stage III, damage in entire cartilage layer and fibrocartilage matrix changes; and stage IV, defects of the entire cartilage extending into subchondral bone. Three to four non-adjacent sections were assessed for each joint, bilaterally.

Statistical analysis

For statistical analyses of the histological data, mixed model ANOVAs were used in which the 3 microscopic observations per muscle, per limb, were used as the blocking factor in the CTGF and collagen type I analyses; the 35 – 50 observations per muscle, per limb, were used as the blocking factor in the myofiber diameter analyses. Counts from the two hind limbs per rat were kept separate for these analyses. Two-way ANOVAs with the factors group (CONT, PA, SR, and PA+SR) and muscle (see next) were used to determine the treatment effect on myofiber diameter, percent area fraction of CTGF, or collagen type I immunoreactive product within each muscle. Percent area fraction of CTGF and collagen were determined in 4 muscles (triceps surae, quadriceps femoris, hamstrings, and gluteus maximus). Myofiber diameters were measured in all but the gluteus maximus due to its curved anatomical shape (rather than straight) which prevented us from having enough longitudinally oriented myofibers in the sections to complete this analysis. Bonferroni post hoc analyses were carried out and adjusted p values reported. These post hoc analyses compared the percent area of CTGF or collagen type I immunoreactivity, or myofiber diameter in the treatment groups (PA, SR, PA+SR) to control tissues, by individual muscle examined. A p value of ≤ 0.05 was considered significant for the tissue analyses.

For the S1 cortical map data, Canvas software was used to calculate the areal extent of each region of the cutaneous map. Cortical zones were described by their absolute areas (mm^2) for each rat. Average values were computed for each group of rats. Since several RFs encompassed glabrous and dorsal foot skin, the absolute size of RFs, measured in mm^2, was normalized relative to the sum of ventral and dorsal foot skin surfaces, and expressed in percentages. The relative RF areas measured in each rat were averaged and the mean size of the RFs was calculated for each group of rats. The RF average size in each rat was calculated by including or not the large RFs located on the dorsum surface of the foot. Statistical treatment of S1 map data was done with non-parametric Mann–Whitney U-test and Chi square (Statistica, Statsoft).

Results

Effects of asphyxia and sensorimotor restriction on hind limb muscles

Previous studies have shown that denervation as well as limb disuse can alter muscle fiber diameters and interstitial connective tissues between muscle fibers (Scelsi et al., 1984; Marbini et al., 2002; Zarzhevsky et al., 2001). We found that myofiber diameters were differentially affected by the three experimental treatments in the three hind limb muscles examined, each of which is critical to rat locomotion: the quadriceps (knee extensor), the hamstrings (knee flexors) and the triceps surae (knee and ankle plantar flexors). ANOVA results examining myofiber diameter showed significant differences between groups ($p \leq 0.001$), between muscles ($p \leq 0.001$), and group by muscle ($p \leq 0.001$). Fig. 1A shows the results of the post hoc analyses. In PA rats, hamstring myofibers increased (indicative of hypertrophy), while quadriceps myofiber diameters decreased (indicative of atrophy) compared to controls. In sensorimotor restricted (SR) rats, only the triceps surae myofibers were affected, showing a significant reduction in mean diameter compared to both control and PA rats. In contrast, in rats exposed to both perinatal asphyxia and sensorimotor restriction (PA+SR), both the triceps surae and quadriceps myofiber diameters were reduced compared to control rats and compared to PA rats, while the hamstring myofibers were significantly reduced compared to PA rats only. Bin frequency histograms were used to further evaluate the atrophy observed in the triceps surae (Fig. 1B). According to Johnson and Kucukyalcin (1978), myofiber diameters smaller than 10 μm represent an index of myofiber atrophy. Atrophied myofibers (≤ 10 μm in diameter) were present in the triceps surae of each treatment group. The most dramatic outcomes were seen in the SR rats exhibiting a loss of all myofiber over 60 μm, while PA+SR rats exhibited a loss of myofibers in the 80 or 100 μm size bins. These losses were not observed in the PA only rats.

Muscle fiber atrophy was accompanied by connective tissue changes in the muscles. Analysis of CTGF and collagen immunoexpression using ANOVA showed a significant increase in CTGF across groups ($p = 0.0252$), but not between the 4

muscles examined (gluteus maximus, triceps surae, hamstrings and quadriceps were each utilized for this analysis). Therefore, the individual muscle data was combined for post hoc analyses (Fig. 1C). The percent area with CTGF was significantly increased in PA+SR rats compared to controls ($p=0.0038$), while the percent area with collagen type I also increased significantly in PA+SR rats compared to controls ($p=0.0047$), and to PA rats ($p=0.0026$).

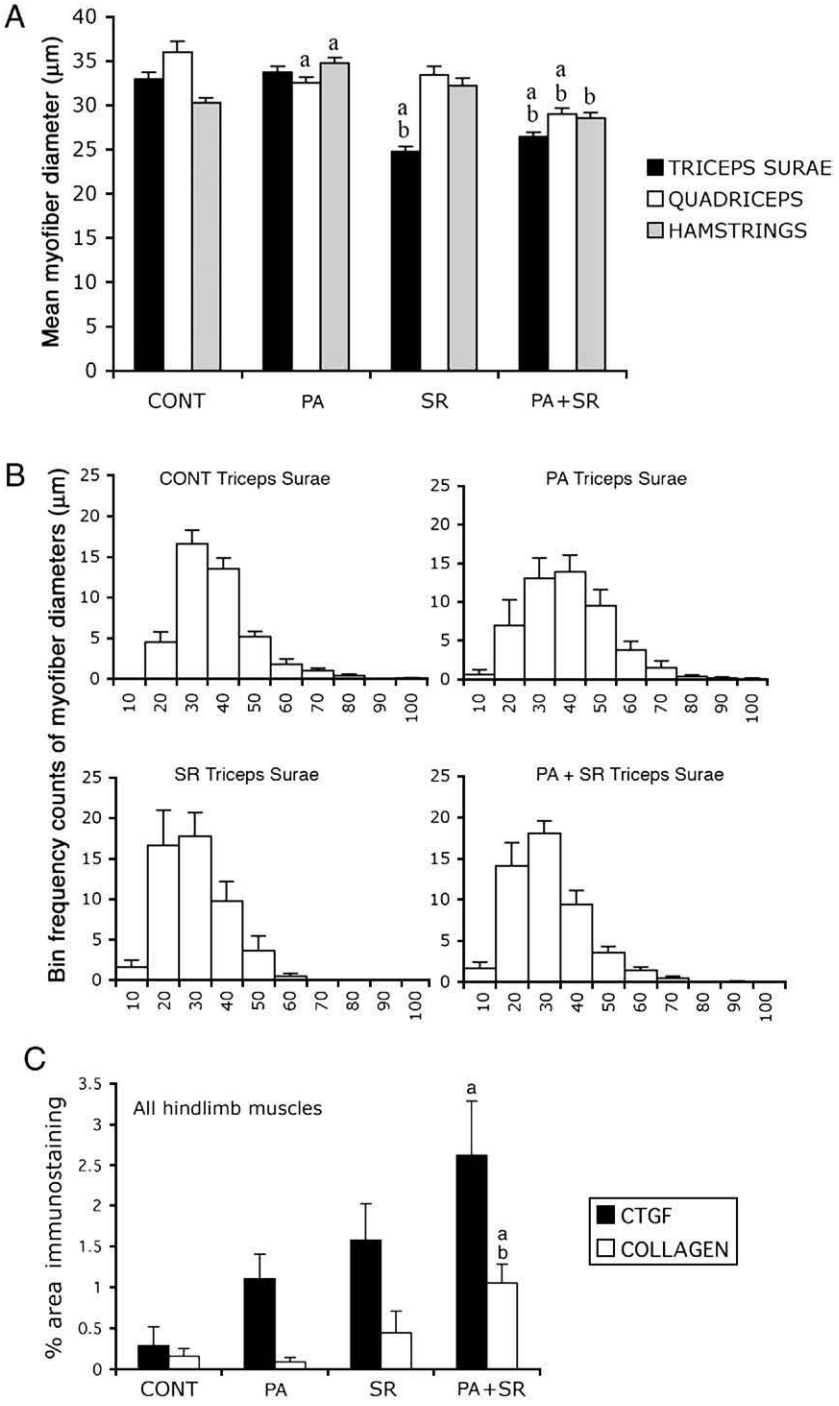

Fig. 1. Graphs showing effects of perinatal asphyxia (PA), sensorimotor restriction (SR), or both (PA+SR) on hind limb myofiber diameters, connective tissue growth factor (CTGF), and collagen type I immunohistochemistry compared to control (CONT) rats. (A) Mean myofiber diameter of 3 hind limb muscles. PA rats had increased myofiber diameters in hamstrings but reduced in quadriceps; SR rats had reduced myofiber diameters in the triceps surae only. In contrast, in the PA+SR group, the myofiber diameters of the three muscles examined were reduced compared to controls (indicated by a), compared to PA only (indicated by b), or compared to both (indicated by a,b). (B) Bin frequency histograms of myofiber diameters of triceps surae muscle. Each of the PA, SR and PA+SR muscles contained atrophied myofibers (≤ 10 μm). (C) Graph showing mean percent area with CTGF and collagen type I immunostaining in four hind limb muscles combined (gluteus maximus, triceps surae, quadriceps and hamstrings). Both CTGF and collagen type I were significantly elevated above control levels in PA+SR rats; collagen type I was also elevated in PA+SR rats compared to PA only rats. Mean+SEM is shown. a: $p \leq 0.001$ compared to controls. b: $p \leq 0.001$ compared to PA rats.

Figure 2 shows the cellular localization of CTGF and collagen type I immunoreactivity. Little to no CTGF or collagen type I immunoexpression was observed in control muscles (<0.28% as shown in Figs. 1C, 2A and B). Many of the CTGF-immunoreactive cells were small cells surrounding the myofibers in the perimysium and endomysium (Fig. 2C). Most of these small cells appeared to be fibroblasts, known to be CTGF immunoreactive. Figure 2D shows collagen type I immunoexpression within several scattered myofibers, and in the perimysium and endomysium of PA+SR rat hind limb muscle, further confirming the connective tissue matrix changes in the PA+SR rats.

Effects of asphyxia and sensorimotor restriction on hind limb articular cartilage

Asphyxia, restriction, or both combined differentially affected the articular cartilages of knee and ankle joints (Fig. 3; Table 1). Medial menisci of SR rats (not shown) and PA+SR rats were undergoing the initial stages of calcification (Fig. 3B). Eburnations (scored as I), thinning (Fig. 3D) and cartilage tidemark changes (scored as II) were present in knee articular cartilage of PA and PA+SR rats, but not in SR rats or controls (Fig. 3A and C, Table 1). One PA+SR rat also contained fibrocartilage patches (scored as III; Fig. 3D) in its knee articular cartilage (Table 1). In contrast, SR rats showed only condensations in the upper layer of knee cartilage (scored as I). Ankle joint changes were milder and fewer in the PA rats compared to the other treatment groups. Only half of the PA rats had thinned ankle articular cartilages, and only one rat displayed ankle cartilage tidemark changes (Table 1). In contrast to the knee joint, the articular cartilages of ankle joints of many SR rats showed eburnations, tidemark changes, and fibrocartilage degenerative changes, as did PA+SR rats (Fig. 3F and G; Table 1). These degenerative cartilage thickenings were immunoreactive for CTGF (Fig. 3H), indicative of cartilage matrix disruption and reorganization. Thus, the greatest knee joint changes were observed in the PA and PA+SR rats, while the greatest degenerative ankle changes were seen in the SR and the PA+SR rats; only the PA+SR rats showed changes in both the knee and ankle joints.

Influence of neonatal asphyxia on the S1 hind limb maps

Electrophysiological S1 maps of the hind limb skin representation obtained in 26 rats (7 CONT, 7 PA, 6 SR and 6 PA+SR) were located between −1 and +3 mm from bregma in the rostrocaudal axis and between 1 and 4 mm in the mediolateral direction. Our maps were derived from a total of 2627 electrode recordings, averaging 101±19 (mean±SD) cortical penetrations per animal.

Despite idiosyncratic differences, the S1 hind limb representation in controls (CONT) presented common somatotopic features. The hind paw representation was usually located

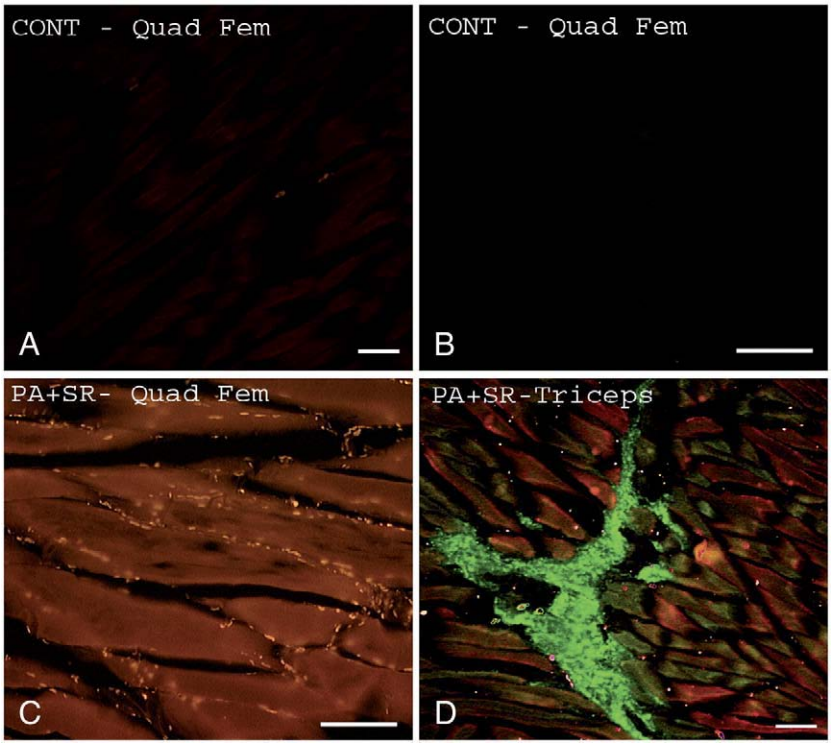

Fig. 2. Photomicrographs showing connective tissue growth factor (CTGF; red) and collagen type I (green) immunoreactivity in hind limb muscles from control (CONT) and perinatal asphyxia plus disuse (PA+SR) rats. Longitudinal sections are shown in A–C; a cross-section in D. (A,B) No CTGF (A) or collagen (B) immunostaining was found in control quadriceps femoris (Quad Fem). (C) Immunostaining in PA+SR rat quadriceps femoris shows increased CTGF-positive cells that appeared to be fibroblasts by location, size, and CTGF production. (D) PA+SR triceps surae double-labeled for both CTGF and collagen type I. Increased collagen type I immunostaining is visible in the endomysium and perimysium. Panels A, B, C: 300×; Panel D: 600×.

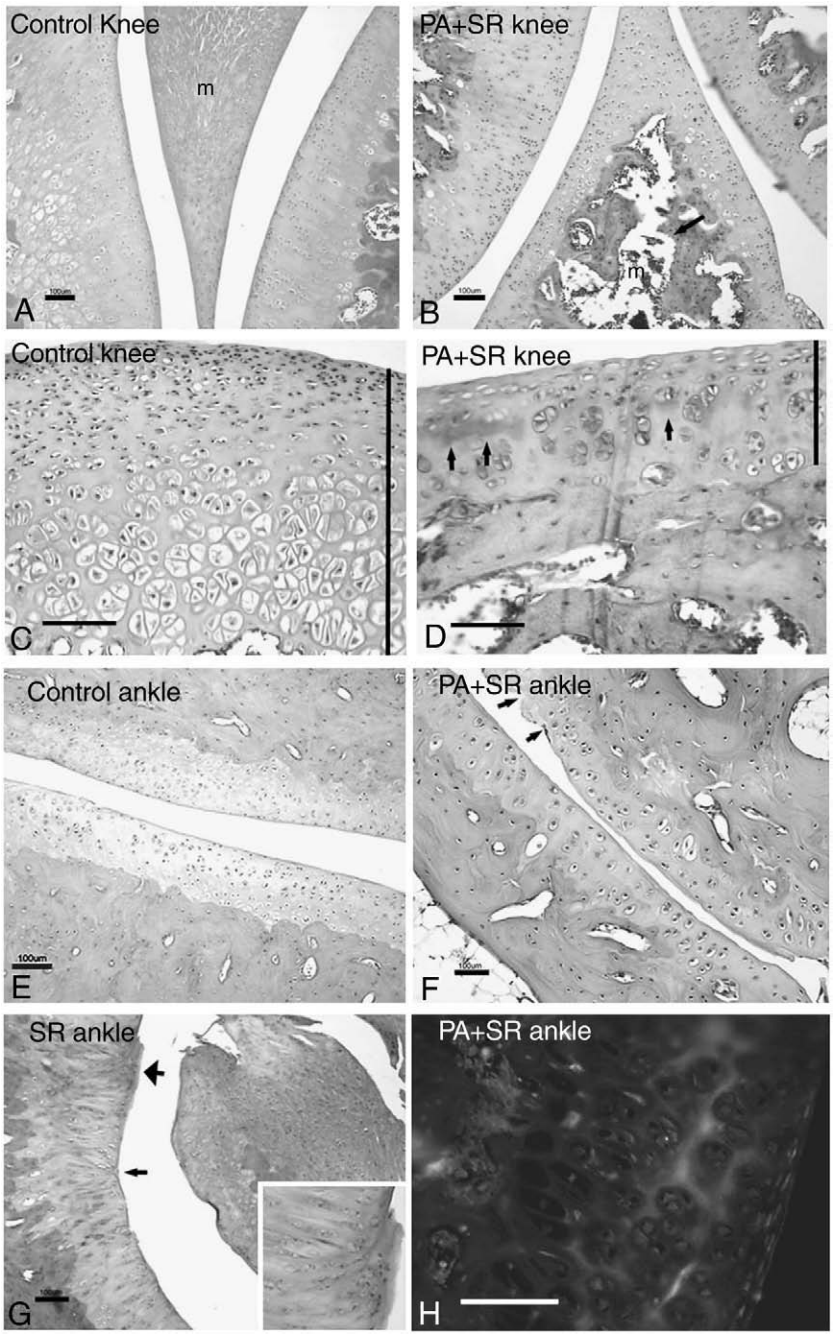

Fig. 3. Photos of knee (A–D) and ankle (E–H) joints from control (CONT), asphyxia plus restraint (PA+SR), and restricted (SR) rats. (A) Control knee joint showing the femur (left) and tibial articular cartilage (right), and medial meniscus (m). (B) PA+SR knee joint showing calcification of the medial meniscus (arrow). (C) Higher power photo of a control knee joint showing a thick (see black bar at right) healthy articular cartilage. (D) Higher power photomicrograph of a PA+SR knee joint showing a thinner articular cartilage than shown in C, and matrix thickening (arrows). (E) Control subtalar joint showing healthy articular cartilage. (F) PA+SR subtalar joint showing eburnations (arrows) in superficial cartilage and tidemark changes (area between cartilage and subchondral bone). (G) SR talotibial joint showing eburnations (small arrow) in superficial cartilage, tidemark changes, and fibrotic cartilage (large arrow). Inset shows a higher power of fibrotic area. (H) PA+SR talotibial joint showing increased CTGF secreted into the cartilage matrix, indicative of matrix disruption. Panels C and D: 300×. Panels A–G: Hematoxylin and eosin staining. Scale bars correspond to 100 μm.

medial to the forepaw map and rostral to the tail and back/ventrum representations. From rostral to caudal, cortical sites progressed from the toes, plantar pads of the sole to the heel and leg. From lateral to medial in the rostral portion of the hind paw map, the toes were topographically represented from toe 1 (t1) to toe 5 (t5) (Fig. 4A). The hairy representation of the toes was generally located medially (t1 to t3, innervated by the saphenous nerve) and laterally (t3 to t5, innervated by the sciatic nerve) to the glabrous representation of the toes (innervated by the sciatic nerve).

The overall and detailed topographic organization of the hind paw representation of asphyxiated (PA) rats did not differ

Table 1
Assessment of articular cartilage using Okabe (1989) classification system

Group	Knee joint cartilage (femur+tibial)		Ankle joint cartilage (talotibial and tarsal joints)	
	Score	% rats	Score	% rats
CONT (n=7)	0	0% (0/13 knees)	0	5% (0/12 ankles)
PA (n=5)	0	25% (2/8 knees)	0	37% (3/8 ankles)
	I	25% (2/8 knees)	I	50% (4/8 ankles)
	II	50% (4/8 knees)	II	13% (1/8 ankles)
SR (n=4)	0	50% (4/8 knees)	0	25% (2/8 ankles)
	I	50% (4/8 knees)	I	25% (2/8 ankles)
			II	37% (3/8 ankles)
			III	13% (1/8 ankles)
PA+SR (n=8)	0	31% (4/13 knees)	0	25% (3/12 ankles)
	I	23% (3/13 knees)	I	25% (3/12 ankles)
	II	46% (6/13 knees)	II	42% (5/12 ankles)
	III	7% (1/13 knees)	III	8% (1/12 ankles)

I=damage in superficial cartilage layer; II=damage in cartilage down to the tidemark; III=damage in entire cartilage layer.

particularly from controls (Fig. 4A and B). The total cortical area of the foot map in PA ($1.09\pm0.33mm^2$) rats was similar to that of CONT ($1.38\pm0.46mm^2$; U=10.0; p: n.s., Table 2), as well as the cortical areas serving either the glabrous or hairy skin surfaces of the hind paw (U=12.5, U=13.5; p: n.s., respectively; Table 2). However, the cortical sites responding to both cutaneous stimulations and nail movements were more numerous in PA than in CONT (χ^2=5.78; p<0.02; Table 3).

The proportions of cortical sites with single, double, triple or more RFs did not differ between the PA and CONT groups (χ^2=6.41; p: n.s.; Table 3). In addition, the mean relative sizes of RFs with or without the large RFs located on the foot dorsum were similar for both groups of rats (U=19.0; p: n.s.; Fig 4, Table 2). Like in CONT, there were no RFs located on both glabrous and hairy foot surfaces in PA rats, nor on both sides of the leg (Fig. 4A and B; Table 3).

Cortical responsiveness to light tactile stimulation was classified, as in our previous studies (e.g. Coq and Xerri, 1999), along a three-level scale (weak, good and excellent responses) on the basis of the magnitude of the signal-to-noise ratio. The cortical responsiveness did not differ between both groups (χ^2=4.09; p: n.s.; Table 3), even when only the most contrasted responses (weak and excellent) were compared (χ^2=2.52; p: n.s.) since the clear responses were dominant (Table 3). Thus, the organizational topography and features of the S1 hind paw maps were relatively similar between asphyxiated only and control rats, as well as the neuronal properties, except for responsiveness to both cutaneous stimuli and nail movements.

Effects of sensorimotor restriction with or without asphyxia on the S1 hind limb representation

Disuse induced a topographical disorganization of the S1 foot maps, which was more severe when combined with PA. The overall somatotopy of the foot maps was preserved in restrained only (SR), but not in asphyxiated and restrained (PA+SR) rats in which the representation of contiguous skin surfaces of the foot was drastically disrupted (Fig. 4).

The total cortical area of the foot was smaller in PA+SR ($0.88\pm0.22mm^2$) rats than in CONT ($1.38\pm0.46mm^2$; U=5.0; p<0.04; Table 2), whereas it did not differ between the PA+SR rats and the PA (U=13.0; p: n.s.) or SR rats (U=10.0; p: n.s.; Table 2). In addition, the total cortical area was not statistically different between SR and CONT (U=8.0; p: n.s.). The cortical area serving the glabrous foot surfaces did not differ between all rats, but tended to be smaller in PA+SR rats than in CONT (U=7.0; p=0.07; Table 2). We found the same results for the cortical area serving the hairy foot skin.

The proportions of cortical sites responding to both hind paw cutaneous stimulation and nail movements were about twice in SR than in CONT (χ^2=21.83; p<0.0001), more than twice in PA+SR compared to CONT (χ^2=34.64; p<0.0001; Table 3). These cortical sites were more numerous in PA+SR than in PA rats (χ^2=14.77; p<0.0001), but did not differ between SR and PA+SR rats (χ^2=0.96; p: n.s.; Table 3). These results show a change in neuronal selectivity between cutaneous and nail movement inputs and emphasize the sensorimotor restriction-induced alterations of the S1 neuronal properties.

The proportions of cortical sites with at least three multiple RFs were 14 and 24 times greater in the SR and PA+SR rats than in controls, respectively (χ^2=399.68; p<0.0001; Table 3). In addition, the proportions of multiple RFs ($\geq$3) were greater in PA+SR than in SR rats (U=19.34; p<0.002), while the percentages of double RFs did not differ between all groups (Table 3). As the numbers of multiple RFs increased with SR in combination to asphyxia or not, the RF size also increased in these experimental groups (Fig. 4). The sizes of all RFs were about twice as large in SR and PA+SR as in CONT (U=1.0; p<0.005 and U=3.0; p<0.01, respectively) or PA (U=2.0; p<0.007; Table 2). However, the RF size was similar between SR and PA+SR rats (U=13.0; p: n.s.). We found similar results for RF sizes when the large RFs located on the foot dorsum were discarded (Table 2). The enlargement of RFs led to a greater overlap between glabrous RFs and a coarser-grained representation of these surfaces in SR and PA+SR rats (Fig. 4).

Figure 4 also illustrates the patchy representations of the glabrous and hairy foot surfaces in the PA+SR rats, which were even more patchy than in the SR rats. To better understand the topographic disruption of the S1 foot maps, the proportions of RFs that encompass both glabrous and hairy foot surfaces were greater in SR and PA+SR rats than in CONT and PA rats (χ^2=117.33; p<0.0001; Table 3). That proportion of glabrous and hairy RFs was greater in PA+SR rats than that in SR rats (χ^2=14.24; p<0.0002). As a consequence of larger and overlapping RFs, and numerous multiple RFs located on both sides of the foot, the delineation of toe and pad representation borders was difficult in the SR rats and even more in the PA+SR rats, so that penetrations with at least three multiple RFs were pooled together in specific cortical sectors (colored in orange) of the S1 foot maps (Fig. 4). Thus, disuse induced a topographical degradation of the S1 foot maps and alterations of the neuronal properties. These changes were more pronounced when immobilization and neonatal asphyxia were combined.

The proportions of excellent responses were much greater in SR and even more in PA+SR than in CONT and PA, while the

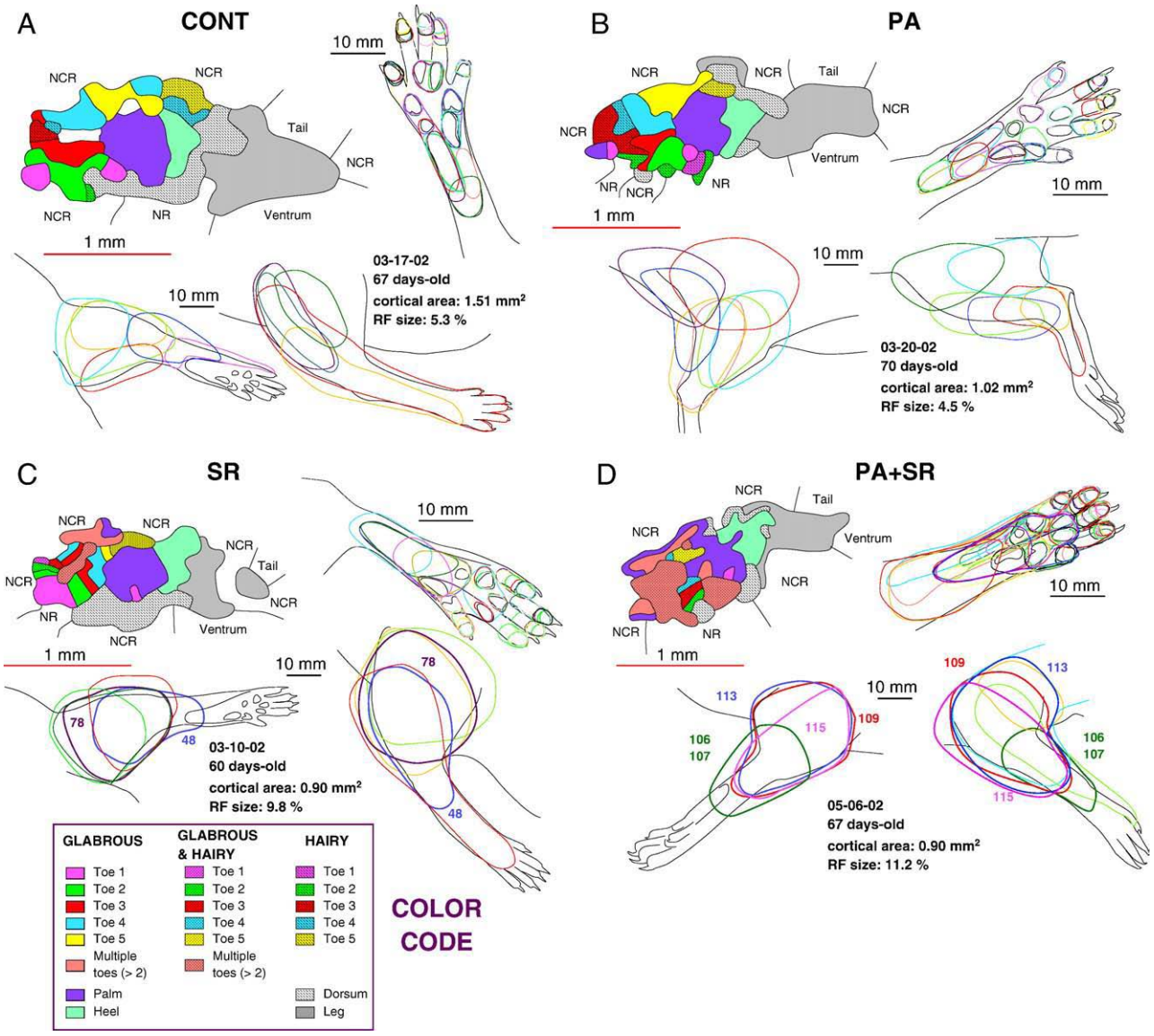

Fig. 4. Effects of neonatal asphyxia and/or disuse during development on the topographical organization of the S1 hind limb maps and RFs. (A) Illustration of the S1 representation of hind paw and of the RFs located on the glabrous foot and leg in a representative control rat (CONT). (B) Example of the S1 hind limb map and RFs in an asphyxiated rat at birth (PA). Topographical organization of S1 maps and RF features are roughly comparable between control and PA rats. (C) Representative S1 map and RFs of the right hind limb in a rat that experienced developmental sensorimotor restriction only (SR). Relative to controls the organization of the S1 foot map was degraded in SR rats and RFs were enlarged. (D) The cortical map of the foot was more degraded in rats asphyxiated at birth and restraint during development (PA+SR) than in SR rats. The cortical area devoted to the whole foot was smaller ($p<0.05$) in PA+SR rats than in CONT. More multiple, large and overlapping RFs were recorded in PA+SR rats than in controls. In addition, we found more RFs encompassing both sides of the foot or leg (illustrated by RF numbers on the leg) in PA+SR rats than in SR rats, while none was encountered in PA and CONT animals.

proportions of weak and clear responses decreased in the former groups ($\chi^2=74.19$; $p<0.0001$; Table 3). However, the different proportions of cortical responsiveness did not differ between the SR and PA+SR rats ($\chi^2=2.72$; p: n.s.). Sensorimotor restriction with or without asphyxia at birth drastically increased the cortical responsiveness to tactile stimulation.

The proportions of RFs covering both sides of the leg were greater in the PA+SR rats (37.3%) than in the SR rats (8.6%; $\chi^2=10.83$; $p<0.001$; Table 3). These RF proportions in both PA+SR and SR were much greater than those in the control and PA rats ($\chi^2=47.51$; $p<0.0001$; Table 3), since no such double-sided RFs were present in the control and PA rats. Thus, sensorimotor restriction alone induced the emergence of RFs located on both sides of the leg, as well as RFs on both glabrous and hairy sides of the foot (see above). In addition, the combination of both experimental paradigms enhanced the most the proportion of this type of RFs.

Discussion

This is the first study to show the deleterious impact of both neonatal asphyxia (PA) and disuse, using a sensorimotor restriction (SR), on the musculoskeletal tissues and S1 hind limb map organization in relation to cerebral palsy. First, we

Table 2
Cortical area occupied by hind limb skin regions and relative sizes of receptive fields in each experimental group

	CONT	PA	SR	PA+SR
Total area (mm^2)	1.38±0.46	1.09±0.33	1.00±0.13	0.88±0.22 [a]
Glabrous skin (mm^2)	0.99±0.36	0.78±0.21	0.75±0.12	0.64±0.12
Hairy skin (mm^2)	0.39±0.13	0.31±0.13	0.26±0.05	0.24±0.11
Leg (mm^2)	0.50±0.23	0.33±0.13	0.21±0.02	0.33±0.09
All RFs (%)	5.90±1.82	5.55±1.83	10.63±1.77 [b]	10.44±3.31 [b]
RFs w/o foot dorsum (%)	4.52±1.41	4.05±0.98	7.04±0.94 [b]	7.88±2.66 [b]

[a] Significantly different from controls, $p<0.05$.
[b] Significantly different from controls and PA rats, $p<0.01$.

found that PA alone increases myofiber size variability (atrophy and hypertrophy of different leg muscles), induces mild to moderate knee and ankle cartilage joint degeneration, no changes in the S1 topographical organization and features of the hind limb maps, but increases the number of cortical sites responding to both cutaneous and proprioceptive (nail movements) inputs. Second, SR alone resulted in distinct myofiber atrophy in one muscle, mild knee but moderate ankle joint degeneration, and profound changes in both the topographical organization of hind limb skin representation and the S1 neuronal properties. Third, these peripheral and cortical alterations were even greater when SR and PA were combined. Additionally, the combination of SR and PA was associated with increased collagen and other connective tissue matrix changes in muscle.

Limited effects of perinatal asphyxia on peripheral tissue and cortical reorganization

In the present study, mild to moderate changes were observed in rats that experienced only asphyxia at birth. In a previous study, we found that PA alone led to roughly normal walking patterns, mild increases in muscular tone and resistance to passive movements of the toes but significant motor cortex alteration in the hind limb movement representations (Strata et al., 2004). In the present study, PA had only limited impact on musculoskeletal tissues with mild hypertrophy of hamstrings and mild atrophy of the quadriceps, which could result in a greater knee flexion during locomotion. This result is in accordance with compensatory and more elevated ankle–foot movements, as previously found in PA rats (Strata et al., 2004).

Possible causes of our observed myofiber size variations could be the denervation following brain anoxia, as suggested by Scelsi et al. (1984) in a study in which cerebral vascular accidents were associated with myofiber atrophy. Interestingly, varying patterns of myofiber atrophy–hypertrophy have been reported in patients with CP depending on the muscle examined and the patient clinical status (Castle et al., 1979; Scelsi et al., 1984; Rose et al., 1994). With regard to joint changes, we found that PA alone resulted in mild to moderate degenerative changes in knee and ankle joint cartilages. The joint changes may be the result of mild anoxia-induced chronic spasticity leading to an incongruent distribution of load on the joints (Banks, 1972; Lundy et al., 1998).

Our present results show that PA alone had a limited impact on the S1 hind limb maps. However, PA rats exhibit increased numbers of S1 neurons responding to both cutaneous stimuli and nail movements (proprioceptive inputs), which seems to be concomitant to increased muscular tone of the toes only (see Strata et al., 2004). This increased muscular rigidity of the toes could provide aberrant sensory inputs to S1 neurons and thus increase the nail movement representation.

The discrepancies in findings relative to PA on brain anatomy and function seem to depend mainly on large variations in the type (anoxia or hypoxia combined or not with ischemia followed or not by reperfusion), duration, severity and developmental stage of the insult (Vannucci et al., 1999). PA seems to induce increased activity in open-field (Buwalda et al., 1995; Row et al., 2002; see however Van de Berg et al., 2003) or in spontaneous locomotion (Brake et al., 2000; see however Hoeger et al., 2006) and abnormal motor, social, emotional and behavioral responses (Kohlhauser et al., 1999; Laviola et al., 2004; Hoeger et al., 2006). PA also reduces neurotransmission (GABA, dopamine and excitatory amino acids) in various brain areas, such as the striatum involved in motor control (Bernert et al., 2003; Van de Berg et al., 2003; Gross et al., 2005). Perinatal asphyxia reduces the volume and the number of neurons and glial cells in the entire rat neocortex (Van de Berg et al., 2000; Schwartz et al., 2004; see however Vannucci, 1978), as well as in the S1–M1 cortex (Bernert et al., 2003; Zhuravin et al., 2004), and also induces deficits in myelination and reduced axonal density (Kohlhauser et al., 2000). Neuronal damage in the S1 and M1 cortex related to PA is concomitant with sensorimotor functional deficits, such as decreased movement activity, delayed negative geotropism, decreased capabilities of animals to maintain themselves on a horizontal wire, and impairments in learning new manipulatory movements (Zhuravin et al., 2004). In addition, Strata et al. (2005)

Table 3
Proportions of the different categories of RF features and cortical responsiveness

	CONT		PA		SR		PA+SR	
	n	%	*n*	%	*n*	%	*N*	%
Single RFs	266	69.7	304	69.9	120	47.0 [a]	113	38.8 [a]
Double RFs	109	28.5	110	25.3	69	27.1	53	18.2
Three and more RFs	7	1.8	21	4.8	66	25.9 [a]	125	43.0 [a, c, d]
Total	382	100	435	100	255	100	291	100
Cutaneous and nail movement responses	109	28.5	174	40.0 [b]	146	57.3 [a]	191	65.6 [a, c]
RFs on both glabrous and hairy foot surfaces	8	2.1	17	3.9	32	12.5	84	28.9 [a, c, d]
RFs on both sides of the leg	0	0	0	0	6	8.6	31	37.3 [a, c, d]
RFs on the leg	76		63		70		83	
Weak responses	65	17.0	53	12.2	19	7.5 [a]	16	5.5 [a]
Good responses	180	47.1	224	51.5	98	38.4	98	33.7
Excellent responses	137	35.9	158	36.3	138	54.1 [a]	177	60.8 [a, c]

[a] Significantly different from controls, $p<0.01$.
[b] Significantly different from controls, $p<0.05$.
[c] PA+SR compared to PA, $p<0.01$.
[d] PA+SR compared to SR, $p<0.01$.

have found a reduced processing efficiency in an auditory discrimination task and a degradation of the tonotopic organization in the A1 map of asphyxiated rats at birth. Thus, the PA-related cortical abnormalities, especially in the S1 cortex could explain the somatosensory deficits reported in patients with CP, such as two-point discrimination, stereoagnosis and proprioceptive degradation (Van Heest et al., 1993; see Clayton et al., 2003 for review).

Deleterious impact of disuse with or without PA on hind limb tissues and S1 maps

In the present study, several musculoskeletal changes were detected in rats exposed to SR alone and in combination with PA. SR alone resulted in significant atrophy of a hind limb muscle (the triceps surae, a knee and ankle flexor muscle, which presented with a complete absence of myofibers greater than 60microns), and moderate joint degeneration in ankle but not knee joints. This distinct atrophy may account for the highest degrees of behavioral and motor cortical degradation observed in SR rats compared to the other groups (see Strata et al., 2004). In contrast, SR combined with PA induced more musculoskeletal changes than SR alone, including atrophy of several muscles involved in knee extension and flexion, and ankle flexion, moderate articular degeneration in both ankle and knee joints, and connective tissue matrix changes in hind limb muscles. It is worth noting that hamstring myofiber hypertrophy, observed in the PA only rats, was cancelled out by the association of PA and SR, suggesting that the observed myofiber enlargements could be due to a compensatory overuse. Myofiber atrophy has been associated with anoxia-induced denervation (Scelsi et al., 1984; Marbini et al., 2002), or as a result of a persistent decrease in muscle activity imposed by contracture or disuse (Lindboe and Platou, 1982; Romanini et al., 1989; Zarzhevsky et al., 2001).

We observed increased CTGF and collagen type I immunoexpression in the PA+SR rat muscles. Levels of CTGF, a cytokine and a growth factor, significantly correlate with fibrotic tissue disorders (Hayashi et al., 2002). It has also been found elevated in tissues of rats affected by repetitive strain injury (Clark et al., 2004). These intrinsic muscle changes may result in stiffening and reduced muscle function, thus perhaps contributing to our observed knee and ankle joint degenerative changes as well as to our previously observed hind limb movement abnormalities (Strata et al., 2004). Muscle structural changes have been linked to immobilization as a result of contracture, disuse or restraint (Williams and Goldspink, 1984), and chronic spasticity (Foran et al., 2005). We also found varying degrees of joint degradation in joint cartilages. Interestingly, knee joint cartilages were more affected in both groups exposed to PA, whereas ankle joint cartilages were more altered in the SR rats with or without PA. Lower extremity articular pathologies have been observed as a consequence of muscular contracture and spasticity in patients with CP (Banks, 1972; Morrell et al., 2002; Lundy et al., 1998). In the present study, the knee extensor (quadriceps) atrophy may have an impact on knee joint dynamics affecting its cartilages. The SR rat's ankle joint hyperextension and poor mobility, as previously reported (Strata et al., 2004), is obviously a degrading factor for that particular joint. The combined treatment of asphyxia and disuse/immobilization apparently enhanced the musculoskeletal pathological changes observed from levels produced by either treatment individually.

Disuse alone or associated with PA induces either similar or differential changes in the S1 map features and neuronal properties. Rats that underwent developmental disuse with or without PA exhibited a degraded topography of the S1 maps, characterized by large and abnormally very large RFs, multiple and often overlapping RFs. These disuse-induced RF changes resulted in a disruption of the topographic contiguity of the representation of adjacent skin surfaces by patches of cortical neurons with more than two distinct RFs, leading to a much coarser-grained representation of foot surfaces than control and PA rats. Both groups of restrained rats also displayed comparable decreases in the neuronal selectivity to afferent (cutaneous and nail movements) inputs and similar increases in cortical responsiveness to tactile stimuli. Interestingly, compared to restriction alone the combination of disuse and PA enhanced the S1 map degradation, reduced the total cortical area devoted to the S1 foot representation, increased the topographic disruptions along with much more numerous cortical sites with at least three distinct RFs and increased the number of RFs located on both sides of the hind paw or leg. The peripheral changes observed in PA+SR rats, such as muscle atrophy, fibrotic muscle changes, and joint degeneration, likely resulted in muscle hyperextension, stiffening and reduced motor function, and thus contributed to abnormal movements found previously in PA+SR rats (Strata et al., 2004). These abnormal movements provided aberrant sensorimotor feedback to the S1 and M1 areas, whose organization has been found to be drastically degraded in PA+SR rats.

Previous studies based on disuse during adulthood partially confirm our results. Forepaw immobilization with a plaster cast for 1 or 2 weeks degraded the S1 topographic organization and drastically reduced the contralateral S1 map area while the size of the corresponding RFs was unchanged (Coq and Xerri, 1999). Hind limb unloading for 2 weeks (weight-bearing absence and motor inactivity) also reduced the S1 map but increased the proportion of large foot RFs (Langlet et al., 1999) and induced abnormal locomotor patterns, such as hind limb hyperextension (Canu and Falempin, 1996). Hind limb hyperextension, as well as deficits in gait and locomotion was also reported in rats experiencing disuse with or without PA (Strata et al., 2004). However, the cortical area of the S1 maps was only reduced when disuse was associated with PA, while the foot maps in M1 were more degraded in case of disuse alone than associated with PA (Strata et al., 2004). In addition, we cannot rule out possible effects of restraint-induced stress on S1 map plasticity. However, Coq and Xerri (1999) reported no increase in stress induced by forepaw immobilization in young adult rats and no significant impact of possible stress on the S1 map reorganization.

The presence of abnormally large RFs covering both sides of either the foot or leg in restrained rats and even more in rats that underwent disuse and PA seems in accordance with the level of

spasticity reported in our previous study. Indeed, Strata et al. (2004) found that both groups of restrained rats showed hind limb rigidity and hypertonicity, as well as increased velocity-dependent resistance to passive motion in all joints of the hind limbs, sign of disabling levels of spasticity, as defined by Lance and McLeod (1981). Co-contractions of antagonist muscles of the leg may have induced synchronous activations of cutaneous mechanoreceptors, thus leading to very large RFs covering the entire leg by physiological mechanisms of plasticity (e.g. Wang et al., 1995; Byl et al., 1996, 1997). In the same line, hypertonicity and rigidity of toes and other joints found in both groups of restrained rats (Strata et al., 2004) contributed to increase the S1 nail movement representation, in a larger proportion than in asphyxiated rats (see above), and to decrease neuronal selectivity to afferent inputs in S1.

Interestingly, both groups of restrained rats exhibited increased cortical responsiveness to tactile stimulation. Dupont et al. (2003) found that hind limb unloading for 2weeks increased S1 neuron responsiveness even though the cutaneous threshold was reduced. These authors suggest that such an increase in cortical responsiveness was underlain by a down-regulation of GABAergic activity. Likewise, whisker trimming, nerve transection or partial hind limb deafferentation led to a marked, but reversible reduction of GAD (gamma amino decarboxylase) immunostaining within layer IV of the cortical zone representing the deprived body part (Warren et al., 1989; Land et al., 1995; Fuchs and Salazar, 1998). Relevant to our study is the observation that reduction in GABAergic inhibition tends also to induce cutaneous RF enlargement, as found in both groups of restraint rats. Such a RF enlargement has been found with micro-iontophoretic injections of bicuculline methiodide to antagonize GABA-mediated inhibition in the cat S1 cortex (Dykes et al., 1984; Alloway et al., 1989).

Functional implications and conclusions

This is the first study to clearly show the deleterious effects of abnormal experience during development, through disuse, on both the peripheral tissue histology and S1 map features. It also shows worsening effects of PA when associated with disuse. In a series of studies, two episodes of asphyxia at birth led to either limited alterations in musculoskeletal tissue and S1 topographic map organization in the present study or modest changes in motor behavior and M1 cortical features (Strata et al., 2004) or drastic effects on auditory behavior and cortical organization (Strata et al., 2005). Since the PA-induced motor dysfunctions previously reported (Strata et al., 2004) did not fit completely the requirements of CP symptoms, it strengthens the idea that neonatal asphyxia in our series of experiments was not the most adapted (see Vannucci, 1978 for review); whereas, other models using perinatal ischemia better reproduced some of the motor and brain dysfunctions and neuro-anatomical abnormalities observed in CP (e.g. Derrick et al., 2004; Haynes et al., 2005; Olivier et al., 2005; Drobyshevsky et al., 2007).

Our study confirms and emphasizes the preponderant role of individual experience in shaping body and brain during maturation. Indeed, we showed that abnormal inputs, through disuse, during development induced some of the motor dysfunctions (Strata et al., 2004) and hind limb histopathologies which resemble those observed in patients with CP (Booth et al., 2001; Liptak and Accardo, 2004; Foran et al., 2005). In addition, the presence of abnormal sensorimotor experience has been recently shown in infants with CP (Hadders-Algra, 2004; Einspieler and Prechtl, 2005), with its possible deleterious impact on musculoskeletal tissues (Lieber, 1986) and cortical reorganization in humans (Clayton et al., 2003). Also, studies using a non-human primate model of hand focal dystonia show that stereotypical, repetitive, abnormal hand movements result in a cortical S1 degradation of the hand representation by normal, physiological mechanisms of plasticity (Byl et al., 1996, 1997). It is possible that PA impinges physiological mechanisms of plasticity (see Vannucci et al., 1999 for review) which could even worsen the already deleterious effects of disuse during development, as reported in the present study. Thus, abnormal and limited movements, through hind limb immobilization, may account for the musculoskeletal tissue changes, which in turn contribute to provide repetitive, aberrant sensory inputs to the immature brain. These aberrant inputs result in abnormal sensory feedback leading to S1 and M1 disorganization and consequently to degraded motor function. Therefore, our study emphasizes the preponderant role of early sensorimotor experience and suggests the critical importance for early interventions and sustained activity in CP children and infants to hopefully restore sensorimotor functions or at least prevent further degradations (Damiano, 2006).

Acknowledgments

The authors would like to thank Mamta Amin and Shreya Amin at Temple University for their assistance with the sectioning and the immunohistochemistry, and Lucas Zier, Jonathan Overdevest, Jonathan Davis and Jessica Tweed for their help in data collection and analysis. This work was supported by the Sandler Foundation, National Institute of Health (Grant NS-10414), Temple University, National Institute of Occupational Health and Safety (Grant OH 03970-04), Fondation NRJ — Fondation de France, CNRS and Ministère de l'Enseignement Supérieur et de la Recherche. F.S. was partly supported by a HFSP long-term fellowship LT 00743/1998-B and partly by personal fundings.

Appendix A. Supplementary data

Supplementary data associated with this article can be found, in the online version, at doi:10.1016/j.expneurol.2007.10.006.

References

Alloway, K.D., Rosenthal, P., Burton, H., 1989. Quantitative measurements of receptive field changes during antagonism of GABAergic transmission in primary somatosensory cortex of cats. Exp. Brain Res. 78, 514–532.

Banks, H.H., 1972. The knee and cerebral palsy. Orthop. Clin. North. Am. 3, 113–129.

Bernert, G., Hoeger, H., Mosgoeller, W., Stolzlechner, D., Lubec, B., 2003. Neurodegeneration, neuronal loss, and neurotransmitter changes in the adult guinea pig with perinatal asphyxia. Pediatr. Res. 54, 523–528.

Blomgren, K., Hagberg, H., 2006. Free radicals, mitochondria, and hypoxia-ischemia in the developing brain. Free Radic. Biol. Med. 40, 388–397.

Booth, C.M., Cortina-Borja, M.J., Theologis, T.N., 2001. Collagen accumulation in muscles of children with cerebral palsy and correlation with severity of spasticity. Dev. Med. Child. Neurol. 43, 314–320.

Bouet, V., Gahery, Y., Lacour, M., 2003. Behavioural changes induced by early and long-term gravito-inertial force modification in the rat. Behav. Brain Res. 139, 97–104.

Brake, W.G., Sullivan, R.M., Gratton, A., 2000. Perinatal distress leads to lateralized medial prefrontal cortical dopamine hypofunction in adult rats. J. Neurosci. 20, 5538–5543.

Byl, N.N., Merzenich, M.M., Jenkins, W.M., 1996. A primate genesis model of focal dystonia and repetitive strain injury: I. Learning-induced dedifferentiation of the representation of the hand in the primary somatosensory cortex in adult monkeys. Neurology 47, 508–520.

Byl, N.N., Merzenich, M., Cheung, S., Bedenbaugh, P., Jenkins, W., 1997. A primate genesis model of focal dystonia and repetitive strain injury: II. The effect of movement strategy on the de-differentiation of the hand representation in the primary somatosensory cortex in adult monkeys. Phys. Ther. 77, 269–284.

Buwalda, B., Nyakas, C., Vosselman, H.J., Luiten, P.G., 1995. Effects of early postnatal anoxia on adult learning and emotion in rats. Behav. Brain Res. 67, 85–90.

Canu, M.H., Falempin, M., 1996. Effect of hind limb unloading on locomotor strategy during treadmill locomotion in the rat. Eur. J. Appl. Physiol. Occup. Physiol. 74, 297–304.

Castle, M.E., Reyman, T.A., Schneider, M., 1979. Pathology of spastic muscle in cerebral palsy. Clin. Orthop. Relat. Res. 142, 223–232.

Clark, B.D., Al-Shatti, T.A., Barr, A.E., Amin, M., Barbe, M.F., 2004. Performance of a high-repetition, high-force task induces carpal tunnel syndrome in rats. J. Orthop. Sports Phys. Ther. 34, 244–253.

Clayton, K., Fleming, J.M., Copley, J., 2003. Behavioral responses to tactile stimuli in children with cerebral palsy. Phys. Occup. Ther. Pediatr. 23, 43–62.

Coq, J.O., Xerri, C., 1999. Tactile impoverishment and sensory-motor restriction deteriorate the forepaw cutaneous map in the primary somatosensory cortex of adult rats. Exp. Brain Res. 129, 518–531.

Damiano, D.L., 2006. Activity, activity, activity: rethinking our physical therapy approach to cerebral palsy. Phys. Ther. 86, 1534–1540.

Derrick, M., Luo, N.L., Bregman, J.C., Jilling, T., Ji, X., Fisher, K., Gladson, C.L., Beardsley, D.J., Murdoch, G., Back, S.A., Tan, S., 2004. Preterm fetal hypoxia-ischemia causes hypertonia and motor-deficits in the neonatal rabbit: a model for human cerebral palsy? J. Neurosci. 24, 24–34.

Drobyshevsky, A., Derrick, M., Wyrwicz, A.M., Ji, X., Englof, I., Ullman, L.M., Zelaya, M.E., Northington, F.J., Tan, S., 2007. White matter injury correlates with hypertonia in an animal model of cerebral palsy. J. Cereb. Blood Flow Metab. 27, 270–281.

Dupont, E., Canu, M.H., Falempin, M., 2003. A 14-day period of hindpaw sensory deprivation enhances the responsiveness of rat cortical neurons. Neuroscience 121, 433–439.

Durand, M., Sarrieau, A., Aguerre, S., Mormede, P., Chaouloff, F., 1998. Differential effects of neonatal handling on anxiety, corticosterone response to stress, and hippocampal glucocorticoid and serotonin (5-HT)2A receptors in Lewis rats. Psychoneuroendocrinology 23, 323–335.

Dykes, R.W., Landry, P., Metherate, R., Hicks, T.P., 1984. Functional role of GABA in cat primary somatosensory cortex: shaping receptive fields of cortical neurons. J. Neurophysiol. 52, 1066–1093.

Einspieler, C., Prechtl, H.F., 2005. Prechtl's assessment of general movements: a diagnostic tool for the functional assessment of the young nervous system. Ment. Retard. Dev. Disabil. Res. Rev. 11, 61–67.

Foran, J.R., Steinman, S., Barash, I., Chambers, H.G., Lieber, R.L., 2005. Structural and mechanical alterations in spastic skeletal muscle. Dev. Med. Child Neurol. 47, 713–717.

Fuchs, J.L., Salazar, E., 1998. Effects of whisker trimming on GABAA receptor binding in the barrel cortex of developing and adult rats. J. Comp. Neurol. 395, 209–216.

Gormley Jr, M.E., 2001. Treatment of neuromuscular and musculoskeletal problems in cerebral palsy. Pediatr. Rehabil. 4, 5–16.

Gross, J., Andersson, K., Chen, Y., Muller, I., Andreeva, N., Herrera-Marschitz, M., 2005. Effect of perinatal asphyxia on tyrosine hydroxylase and D2 and D1 dopamine receptor mRNA levels expressed during early postnatal development in rat brain. Brain Res. Mol. Brain Res. 134, 275–281.

Hadders-Algra, M., 2004. General movements: a window for early identification of children at high risk for developmental disorders. J. Pediatr. 145, S12–S18.

Hayashi, N., Kakimuma, T., Soma, Y., Grotendorst, G.R., Tamaki, K., Harada, M., Igarashi, A., 2002. Connective tissue growth factor is directly related to liver fibrosis. Hepatogastroenterology 49, 133–135.

Haynes, R.L., Baud, O., Li, J., Kinney, H.C., Volpe, J.J., Folkerth, D.R., 2005. Oxidative and nitrative injury in periventricular leukomalacia: a review. Brain Pathol. 15, 225–233.

Hill, A., Volpe, J.J., 1989. Perinatal asphyxia: clinical aspects. Clin. Perinatol. 16, 435–457.

Hoeger, H., Engidawork, E., Stolzlechner, D., Bubna-Littitz, H., Lubec, B., 2006. Long-term effect of moderate and profound hypothermia on morphology, neurological, cognitive and behavioural functions in a rat model of perinatal asphyxia. Amino Acids 31, 385–396.

Jarvinen, T.A., Jozsa, L., Kannus, P., Jarvinen, T.L., Jarvinen, M., 2002. Organization and distribution of intramuscular connective tissue in normal and immobilized skeletal muscle. An immunohistochemical, polarization and scanning electron microscopic study. J. Muscle Res. Cell Motil. 23, 245–254.

Johnson, M.A., Kucukyalcin, D.K., 1978. Patterns of abnormal histochemical fibre type differentiation in human muscle biopsies. J. Neurol. Sci. 37, 159–178.

Kohlhauser, C., Kaehler, S., Mosgoeller, W., Singewald, N., Kouvelas, D., Prast, H., Hoeger, H., Lubec, B., 1999. Histological changes and neurotransmitter levels three months following perinatal asphyxia in the rat. Life Sci. 64, 2109–2124.

Kohlhauser, C., Mosgoller, W., Hoger, H., Lubec, B., 2000. Myelination deficits in brain of rats following perinatal asphyxia. Life Sci. 67, 2355–2368.

Lance, J.W., McLeod, J.G., 1981. A Physiological Approach to Clinical Neurology, 3rd Ed. Butterworths, London.

Land, P.W., De Blas, A.L., Reddy, N., 1995. Immunocytochemical localization of GABAA receptors in rat somatosensory cortex and effects of tactile deprivation. Somatosens. Res. 12, 127–141.

Langlet, C., Canu, M.H., Falempin, M., 1999. Short-term reorganization of the rat somatosensory cortex following hypodynamia–hypokinesia. Neurosci. Lett. 266, 145–148.

Laviola, G., Adriani, W., Rea, M., Aloe, L., Alleva, E., 2004. Social withdrawal, neophobia, and stereotyped behavior in developing rats exposed to neonatal asphyxia. Psychopharmacology (Berl.) 175, 196–205.

Lieber, R.L., 1986. Skeletal muscle adaptability. I: review of basic properties. Dev. Med. Child Neurol. 28, 390–397.

Lindboe, C.F., Platou, C.S., 1982. Disuse atrophy of human skeletal muscle. An enzyme histochemical study. Acta Neuropathol. (Berl.) 56, 241–244.

Liptak, G.S., Accardo, P.J., 2004. Health and social outcomes of children with cerebral palsy. J. Pediatr. 145, S36–S41.

Lundy, D.W., Ganey, T.M., Ogden, J.A., Guidera, K.J., 1998. Pathologic morphology of the dislocated proximal femur in children with cerebral palsy. J. Pediatr. Orthop. 18, 528–534.

Marbini, A., Ferrari, A., Cioni, G., Bellanova, M.F., Fusco, C., Gemignani, F., 2002. Immunohistochemical study of muscle biopsy in children with cerebral palsy. Brain Dev. 24, 63–66.

Meaney, M.J., Aitken, D.H., Viau, V., Sharma, S., Sarrieau, A., 1989. Neonatal handling alters adrenocortical negative feedback sensitivity and hippocampal type II glucocorticoid receptor binding in the rat. Neuroendocrinology 50, 597–604.

Morrell, D.S., Pearson, J.M., Sauser, D.D., 2002. Progressive bone and joint abnormalities of the spine and lower extremities in cerebral palsy. Radiographics 22, 257–268.

Myers, R.E., 1975. Four patterns of perinatal brain damage and their conditions of occurrence in primates. Adv. Neurol. 10, 223–234.

Nelson, K.B., Grether, J.K., 1999. Causes of cerebral palsy. Curr. Opin. Pediatr. 11, 487–491.

Olivier, P., Baud, O., Evrard, P., Gressens, P., Verney, C., 2005. Prenatal ischemia and white matter damage in rats. J. Neuropathol. Exp. Neurol. 64, 998–1006.

Peterson, B.E., Merzenich, M.M., 1995. MAP: a Macintosh program for generating categorical maps applied to cortical mapping. J. Neurosci. Methods 57, 133–144.

Prechtl, H.F., 1997. State of the art of a new functional assessment of the young nervous system. An early predictor of cerebral palsy. Early Hum. Dev. 50, 1–11.

Romanini, L., Villani, C., Meloni, C., Calvisi, V., 1989. Histological and morphological aspects of muscle in infantile cerebral palsy. Ital. J. Orthop. Traumatol. 15, 87–93.

Rose, J., Haskell, W.L., Gamble, J.G., Hamilton, R.L., Brown, D.A., Rinsky, L., 1994. Muscle pathology and clinical measures of disability in children with cerebral palsy. J. Orthop. Res. 12, 758–768.

Row, B.W., Kheirandish, L., Neville, J.J., Gozal, D., 2002. Impaired spatial learning and hyperactivity in developing rats exposed to intermittent hypoxia. Pediatr. Res. 52, 449–453.

Scelsi, R., Lotta, S., Lommi, G., Poggi, P., Marchetti, C., 1984. Hemiplegic atrophy. Morphological findings in the anterior tibial muscle of patients with cerebral vascular accidents. Acta Neuropathol. (Berl.) 62, 324–331.

Schwartz, M.L., Vaccarino, F., Chacon, M., Yan, W.L., Ment, L.R., Stewart, W.B., 2004. Chronic neonatal hypoxia leads to long term decreases in the volume and cell number of the rat cerebral cortex. Semin. Perinatol. 28, 379–388.

Strata, F., Coq, J.O., Byl, N.N., Merzenich, M.M., 2004. Comparison between sensorimotor restriction and anoxia on gait and motor cortex organization: implications for a rodent model of cerebral palsy. Neuroscience 129, 141–156.

Strata, F., Delpolyi, A.R., Bonham, B.H., Chang, E.F., Liu, R.C., Nakahara, H., Merzenich, M.M., 2005. Perinatal anoxia degrades auditory system function in rats. Proc. Natl. Acad. Sci. U. S. A. 102, 19156–19161.

Van de Berg, W.D., Blokland, A., Cuello, A.C., Schmitz, C., Vreuls, W., Steinbusch, H.W., Blanco, C.E., 2000. Perinatal asphyxia results in changes in presynaptic bouton number in striatum and cerebral cortex—a stereological and behavioral analysis. J. Chem. Neuroanat. 20, 71–82.

Van de Berg, W.D., Kwaijtaal, M., de Louw, A.J., Lissone, N.P., Schmitz, C., Faull, R.L., Blokland, A., Blanco, C.E., Steinbusch, H.W., 2003. Impact of perinatal asphyxia on the GABAergic and locomotor system. Neuroscience 117, 83–96.

Van Heest, A.E., House, J., Putnam, M., 1993. Sensibility deficiencies in the hands of children with spastic hemiplegia. J. Hand. Surg. 18, 278–281.

Vannucci, R.C., 1978. Neurological aspects of perinatal asphyxia. Pediatr. Ann. 7, 15–31.

Vannucci, R.C., Connor, J.R., Mauger, D.T., Palmer, C., Smith, M.B., Towfighi, J., Vannucci, S.J., 1999. Rat model of perinatal hypoxic-ischemic brain damage. J. Neurosci. Res. 55, 158–163.

Wang, X., Merzenich, M.M., Sameshima, K., Jenkins, W.M., 1995. Remodelling of hand representation in adult cortex determined by timing of tactile stimulation. Nature 378, 71–75.

Warren, R., Tremblay, N., Dykes, R.W., 1989. Quantitative study of glutamic acid decarboxylase-immunoreactive neurons and cytochrome oxidase activity in normal and partially deafferented rat hind limb somatosensory cortex. J. Comp. Neurol. 288, 583–592.

Williams, P.E., Goldspink, G., 1984. Connective tissue changes in immobilised muscle. J. Anat. 138 , 343–350.

Yamamoto, K., Shishido, T., Masaoka, T., Imakiire, A., 2005. Morphological studies on the ageing and osteoarthritis of the articular cartilage in C57 black mice. J. Orthop. Surg. 13, 8–18.

Zarzhevsky, N., Menashe, O., Carmeli, E., Stein, H., Reznick, A.Z., 2001. Capacity for recovery and possible mechanisms in immobilization atrophy of young and old animals. Ann. N. Y. Acad. Sci. 928, 212–225.

Zhuravin, I.A., Dubrovskaya, N.M., Tumanova, N.L., 2004. Postnatal physiological development of rats after acute prenatal hypoxia. Neurosci. Behav. Physiol. 34, 809–816.